Journal of Al-Azhar University Engineering Sector

Vol.17, No. 65, October 2022, 1327-1347

OPTIMAL ALLOCATION OF CHARGING STATIONS FOR ELECTRIC VEHICLE IN DISTRIBUTION SYSTEM USING ARTIFICIAL INTELLIGENCE TECHNIQUES

Mohamed Abdelhamed Zaki[1,*], Tarek Mahmoud[2], Mohamed Atia[1], Elsaid Abdelaziz Osman[2]

[1] Department of Electrical Power and Machines., The Higher Institute of Engineering, Elshorouk City, Elshorouk Academy, Cairo, Egypt.

[2] Department of Electrical Engineering., Faculty of Engineering, Al-Azhar University, Cairo, Egypt.

*Corresponding: m.zaky@sha.edu.eg

Received: 20 July 2022 Accepted: 11 August 2022

ABSTRACT

In this paper, two optimal sizing and sitting techniques are proposed for an Electric Vehicle Charging Station (EVCS) on a Distribution System in Elshorouk City, Cairo, Egypt. An improved metaheuristic, named Archimedes Optimization Algorithm (AOA) and Particle Swarm Optimization (PSO) are proposed; to determine the optimal alocations for EVCS considering the objectives of minimizing real power loss, minimizing cost, and maintaning the required voltage profile. In this work, the photovoltaic (PV) is used as a renewable source as a main feeder for the charge stations (CSs). The 46-bus distribution system in Elshorouk City, Cairo, Egypt is testing network as a conducts simulation tests. The results highlight the need of the EVCS sizing and sitting to improve the performance. The optimization technique (AOA) results is compared to the results of the other optimization technique algorithm (PSO). It shows its effectiveness (fast speed, short time and accuracy) and above all gave better power losses and costs as required.

KEYWORDS: Electric Vehicle Charging Station (EVCS), optimal sizing and sitting of EVCS, particle swarm optimization (PSO) and Archimedes optimization algorithm (AOA)

التخصيص الأمثل لمحطات شحن المركبات الكهربية في نظام التوزيع بإستخدام تقنيات الذكاء الأصطناعي

محمد عبد الحميد زكي[١]* ، طارق محمود[٢] ، محمد عطية[١] ، السعيد عبد العزيز عثمان[٢]

[١] قسم الهندسة هندسة القوى والآلات الكهربية , المعهد العالي للهندسة , مدينة الشروق , أكاديمية الشروق , القاهرة , مصر

[٢] قسم الهندسة الكهربية, كلية الهندسة, جامعة الازهر, القاهرة, مصر

*البريد الاليكتروني للباحث الرئيسى: m.zaky@sha.edu.eg

الملخص

في هذه الدراسة ، تم اقتراح تقنيتين مثاليتين لتحديد الحجم ومكان لمحطة شحن السيارات الكهربائية (EVCS) على نظام التوزيع في مدينة الشروق ، القاهرة ، مصر. اقترحت خوارزمية تحسين أرشميدس (AOA) وسرب الجسيمات المحسّنة ؛ لتحديد الموقع والحجم الأمثل لـ EVCS مع الأخذ في الاعتبار أهداف التقليل من فقدان الطاقة الحقيقي ، وتقليل التكلفة ، وتحسين الجهد. في هذا العمل ، استخدمنا مصدر الطاقة الكهروضوئية (PV) المتجدد كمغذي رئيسي لمحطات CS. يختبر نظام توزيع ٤٦ قضيب في مدينة الشروق ، القاهرة ، مصر. أبرزت النتائج إلى تحديد حجم EVCS ومكانها لتحسين الأداء. تمت مقارنة نتائج تقنية التحسين (AOA) بنتائج خوارزمية تقنية التحسين الأخرى (PSO) ، فقد أظهرت فعاليتها (السرعة والوقت القصير والدقة) وفوق كل ذلك أعطت اقل طاقة مستهلكة واقل تكلفة ممكنة.

الكلمات المفتاحية : محطة شحن السيارة الكهربائية (EVCS) ، أفضل حجم ومكان لـ EVCS ، تحسين سرب الجسيمات (PSO) وخوارزمية ارشميدس (AOA)

1. INTRODUCTION

Today, the world's demand for fossil fuels is increasing in both the transport and power generation sectors, also to greenhouse gas emissions and environmental pollution [1]. According to studies presented in [2], production will rise by 54% in the transport industry by 2035, which will increase prices and air pollution by significant demand. Therefore, many nations are seeking to replace green vehicles instead of internal combustion cars [3]. Electric vehicles (EVs) have shown additional benefits compared with their fossil fuel vehicle counterparts. They produce fewer emissions even when considering their whole process of energy production, independently of their energy source [4]. EV is an up-and-coming solution for the problem of transportation and pollution [5]. The first technology introduced will take place via vehicle-to-grid in 1977 [6]. This promising framework had been first used by the provision of a revenue and expenditure model for regulatory and auxiliary services [7].
Penetrations of electrical vehicles (EVs) in the grid face challenges including thermal limit breaches in certain sensitive network buses of transmission lines because of overload or voltage drop and demand uncertainty [8, 9]. The most popular vehicles in the parking mode are almost 95 % of the day, according to previous studies. Consequently, it can be used this capacity for frequency and voltage regulation through V2G [10]. Vehicle participation in V2G generates money for owners of cars. It can also use to minimize network challenges by using EV and PHEV charging station capabilities [11, 12]. Vehicles will refill batteries at these stations and sell excess stored energy to grid and profit from it. In this situation, it is possible to handle the charging and discharging of vehicles using various approaches, such as adjusting energy tariffs at different time slots.

Literature review many researchers have investigated the design and operation of EV CSs and PV renewable source on the distribution systems and little researcher used the AOA. In [13] the authors used the AOA to chose the optimum sizing and siting of EVCS, they used photo voltaic (PV) renewable source as a main feeder for the CSs, used the power losses objective, the used IEEE 33-bus distribution system for testing, and compare between the results by using AOA, CS and PSO. The authors in [14] studied a new optimal allocation and sizing for an Electric Vehicle Charging Station (EVCS) by using Balanced Mayfly Algorithm (BMA) and used Voltage Profile Improvement Index (VPII), Reactive Power Loss Reduction Index (QLRI), Real Power Loss Reduction Index (PLRI), and the preliminary development cost to get the minimum value of the installation cost. The (BMA) applied to 30-bus distribution system in Allahabad, India and its results were compared with GAIPSO and basic MA. The authors in [15] used the AOA to choose the optimum location and capacity of DG and use the power losses as an objective and compared between the results using AOA, IGA and PSO.

In [16] the authors presented an optimization approach to optimally size multiple DGs and SOPs placements via AOA and NR from the planning and operational viewpoints. Case studies conducted on the real distribution networks, including the 59-node distribution network in Cairo and the 135-node distribution network in Brazil, to step on the effectiveness of SOPs insertion in enhancing DGs penetration.

Various EV-PV charger architectures were tested and analyses in [17]. In this review, the charger of EV-PV presented with two optimal designs. The authors in [18] designed of smart charging station implemented in which the charging of the PHEVs controlled to minimize the effect of charging during the peak load period on the grid. The PHEVs paid in that scheme via the PV of grid-connected system and/or the utility a special controller developed to allow effective energy transfer, while at the same time reducing the conversion stage between source and load [19]. The system consists of modules designed to enhance flexibility and encourage development. In an unregulated charging method, the integration of PV and EVs were studied [20].

In [21], the authors presented an optimum configuration, with regard to renewable energy and diesel generation, for an Electric Vehicle Charge Station (EVCS). The goal was the lifecycle cost is reducing, while considering environmental pollution. The authors in [22] presented the option of charging EV on site using an optimized storage power system PV. A comparison between these profiles and between these profiles presented to minimize the reliance on grids and to optimize the use of PV power to charge the electricity directly. Authors in [23] presented the proposed rapid delivery network linked EV-CS model. By reducing harmonic current, the proposed model improves the power efficiency. In order to minimize the effect of fast charging on the grid, a PV power system developed with a strategy focused on optimum power flow EV-CS. In [24] a genetic algorithm used by optimizing benefit determined by its net current value to maximize the installation and activity of EV fast charging. In order to increase the profitability of the stations and decrease the high grid energy requirements, wind, photovoltaic, storage systems connected to EV-CS.

The main contributions of this work shown as follows:

1. Discuss the impact of EV-CSs on electric feeder losses by feeding the PV.
2. Detects the optimal allocation of CSs for loss reduction subjected to system constraints.

3. The PSO and AOA techniques used to detect the optimal placement for the CSs.
4. The proposed algorithm applied to a Distribution System in Elshorouk City, Cairo, Egypt, to determine optimum size and location of EV-CS.
5. The results analyzed and compared.

This paper is organized; section two presents the mathematical formulation of the problem. The definition and description of the PSO, and AOA methods introduce in section three. Section four introduces numerical applications and case studies. The results and discussion introduce in section five, whereas section six concludes the paper.

2. PROBLEM FORMULATION

The problem formulates as an optimization for general CSs sizing and sitting considering practical features of CS, the operation, and load restrictions at different rates of the load.

The general proposed methodology for the problem is getting as shown **Fig 1** and next steps:

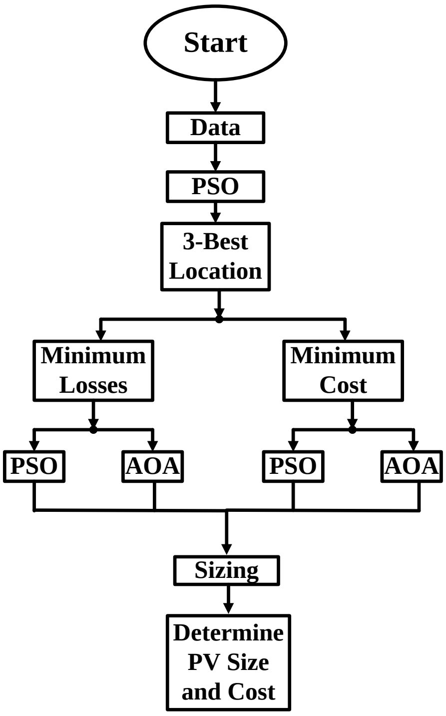

Fig. 1 Flow Chart of general proposed methodology

1. Run base case study
2. Run optimization analysis using PSO algorithm with objective of minimization system losses because to find the optimal locations.
3. Get optimal sitting for the CSs
4. Run optimization analysis using both PSO and AOA algorithms with multi-objective function of minimization system losses and cost.
5. Get optimal sizing for the CSs
6. Determine the PV size which feeding each CS
7. Economical study for PV CS

The optimization problem formulates with a non-differentiable objective function. This paper proposes a solution algorithm depends on PSO and AOA techniques and aims to detect the allocation of CSs. The algorithm can detect the global optimal solution for sitting and sizing of the CSs.

2.1. Objective Function

2.1.1. Minimum Power Losses

The aim of this article is to find the best locations and size of charge station by decreasing the system losses. The problem of optimization is conceived as one purpose function. The calculation of the power loss in the line section connecting buses i and i + 1 before integrating any charging station can be formulated as shown in equation (1) [13]:

$$\mathrm{P_{Loss}}(\mathrm{i.i}+1) = \mathrm{R_i}\left(\frac{\mathrm{P_i^2}+\mathrm{Q_i^2}}{|\mathrm{V_i^2}|}\right) \quad (1)$$

where;

R_i The section line resistance, Ω

P_i Active power of the i^{th} bus, W

Q_i Reactive power of the i^{th} bus, VAR

V_i Voltage of the i^{th} bus, V

The total network losses are calculated as equation (2):

$$P_{TLoss}(i.i+1) = \sum_{i=1}^{n} \mathrm{I_i^2 R_i} \quad (2)$$

where, n is the total line section in the system.

Network losses can be formulated due to the addition of CSs as equation (3) [13]:

$$P'_{TLoss}(i.i+1) = \sum_{i=1}^{n} \mathrm{I_T^2 R_i} \quad (3)$$

where, I_T is the current total line section, including the current charging station.

The PV losses to the charge station are represented in equation (4):

$$P''_{TLoss} = \sum_{i=1}^{n} \left(\mathrm{I_{cs}} - \mathrm{I_{pv}}\right)^2 \mathrm{R_i} \quad (4)$$

where, I_{pv} is photovoltaic current delivered to the CS or the utility.

The proposed objective function can be expressed as equation (5):

$$Min.P_{TLoss} = \sum_{i=1}^{n} \left(I_i + I_{cs} - I_{pv}\right)^2 R_i \quad (5)$$

2.1.2. Minimum Cost

Calculate the cost charging by using equation (6)

$$Cost = \sum_{h=1}^{h=24} RTP_h \times E_{h=1}^{h=24} \quad (6)$$

where RTP= Real Time Pricing [25] and $E = Energy = P * h$

2.2. System Constraints

The maximum and minimum voltage limites at each busbar that is, ± 5% of the nominal value is clear in equation (7).

$$0.95\,pu \le V_i \le 1.05\,pu \quad (7)$$

Line Loading Constraints: maximum and minimum apparent power limites of each line in equation (8).

$$S_{ij\_min} \leq S_{ij} \leq S_{ij\_max} \quad (8)$$

Equation (9), the Capacity Constraints: maximum and minimum limits of each EV-CS capacity.

$$CCS_{k\,min} \leq CCS_k \leq CCS_{k\,max} \quad (9)$$

Active Power Balance Constraints: the total generated active power must equal the demand active power plus the losses shown in equation (10).

$$\mathrm{P_{i+1}} = \mathrm{P_i} - \mathrm{P_{loss.i}} - \mathrm{P_{L.i+1}} \quad (10)$$

Reactive Power Balance Constraints: the total generated reactive power must equal to the demand reactive power plus the losses shown in equation (11).

$$\mathrm{Q_{i+1}} = \mathrm{Q_i} - \mathrm{Q_{loss.i}} - \mathrm{Q_{L.i+1}} \quad (11)$$

The equation (10) and equation (11) can be modelled through the following mathematical relations [13].

$$\mathrm{P_{i+1}} = \mathrm{P_i} - \mathrm{P_{loss.i}} - \mathrm{P_{L.i+1}} = \mathrm{P_i} - \frac{\mathrm{R_i}}{|\mathrm{V_i^2}|}\left(\mathrm{P_i^2} + \left(\mathrm{Q_i} + \mathrm{Y_i}|\mathrm{V_i^2}|^2\right)^2\right) - \mathrm{P_{L.i+1}} \quad (12)$$

$$Q_{i+1} = Q_i - Q_{loss.i} - Q_{L.i+1} = Q_i - \frac{X_i}{|V_i^2|}(P_i^2 + (Q_i + Y_{i1}|V_i^2|^2)^2) - Y_{i1}|V_i^2| - Y_{i2}|V_{i+1}^2| - Q_{L.i+1} \quad (13)$$

$$|V_{i+1}^2| = |V_i^2| + \frac{R_i^2 + X_i^2}{|V_i^2|}(P_i^2 + Q_i^2) - 2(R_iP_i + X_iQ_i) \quad (14)$$

Where,

V_{min}, V_{max} are the minimum and maximum bus voltages,

CCS_k is the capacity of the k^{th} PV charging station,

CCS_{k_min} is the minimum capacity of the k^{th} PV charging station,

CCS_{k_max} is the maximum capacity of the k^{th} PV charging station,

S_{ij} is the apparent power in the line connecting between bus i and bus j,

S_{ij_min} is the minimum apparent power of the line ij,

S_{ij_max} is the maximum apparent power of the line ij,

P_i , Q_i are the real and reactive power flow out of the i^{th} bus,

$P_{L.i+1}$, Q_{Li+1} are the load real and reactive power at bus $i+1$,

R_i , X_i are the section line resistance and reactance respectively.

3. OPTIMIZATION TECHNIQUE

3.1. Particle Swarm Optimization (PSO) algorithm

To determine EV-CS location and sizing, PSO algorithm [13] is applied to optimize the constrained objective function in equation (15) for the case study. The number of variables in the optimization problem is 2.Thus, each particle of swarm searches for optimal result in 2-dimensional search space and it can be represented the particle as:

$$Particle_i = (L_{CS}, P_{CS}) \quad (15)$$

Where, $L_{CS}$is the EV-CS location and P_{CS} is the EV-CS size. The flowchart of optimization technique using PSO is shown in **Fig. 2**.

3.2. Archimedes Optimization Algorithm (AOA)

The Algorithm of Archimedes Optimization (AOA) is a population-based algorithm. In the suggested solution, the submerged objects are the citizens of the population. AOA also begins the search process with the initial population of objects (candidate solutions) with random volumes, densities and accelerations, as other population-based metaheuristic algorithms. Each object is initialized at this stage by its random fluid location. AOA functions in iterations after assessing the fitness of the original population before it satisfies the termination criterion. AOA changes the density and volume of every object at every iteration. Object acceleration is modified depending on the state of its collision with some other adjacent object. The updated density, volume, acceleration determines the new position of an object. Following is the detailed mathematical expression of AOA steps [13].

3.2.1. Algorithmic steps

The AOA algorithm is provided in the mathematical formulation. In theory, AOA is a global optimization algorithm, which involves both discovery and operating processes. Algorithm 2 presents the pseudo-code of the proposed algorithm; including population initialization, population evaluation, and updating parameters. Mathematically, steps of the proposed AOA are detailed in Ref. [13.]

The flowchart of optimization technique using AOA is shown in **Fig. 3**.

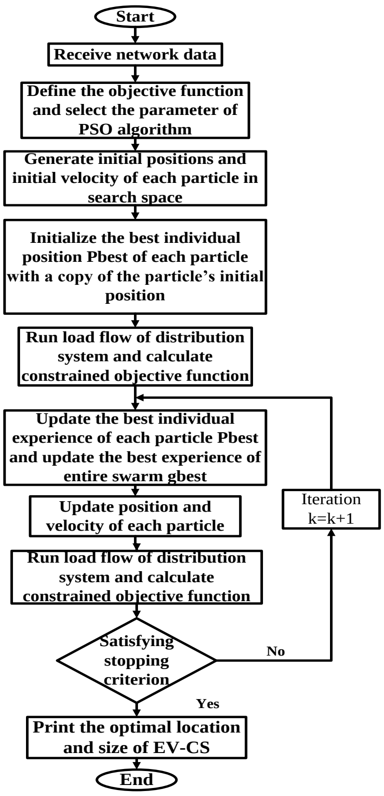

Fig. 2 Flowchart of PSO technique

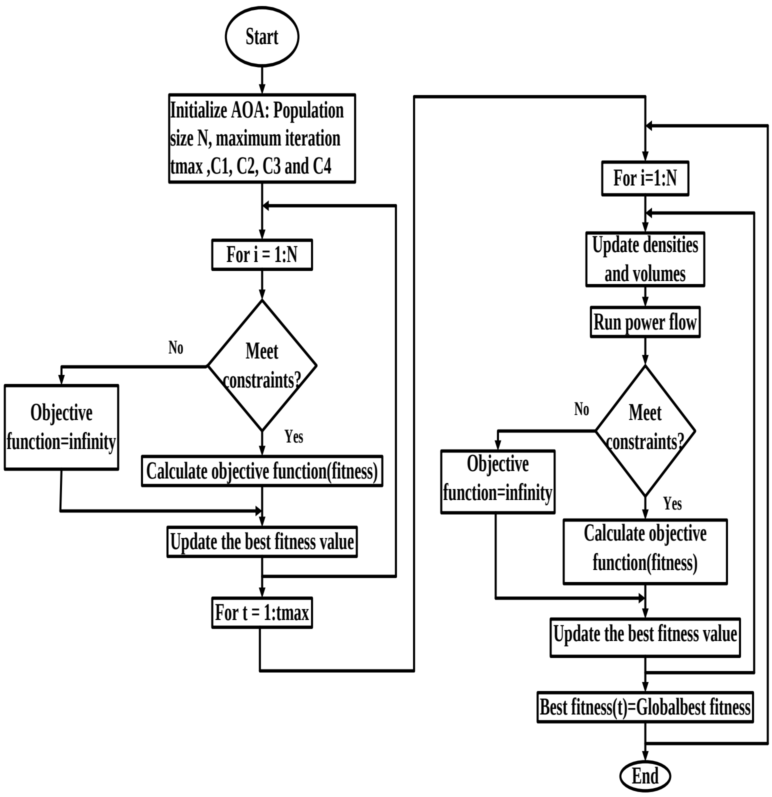

Fig. 3 Flowchart of AOA technique

4. CASE STUDY

4.1. System data

To study the impact of EVs integration on distribution system in Egypt, the distribution system in a District #8 of Shorouk City (ShC-D8) is selected for investigation. ShC distribution network is supplied by Four 66/22 kV, 25 MVA transformers substation. Further distribution of the supply is done from the 22-kV switchgear. The distribution system has both high voltage and low voltage customers via 17 distributers. The distributer (MDE3) located at District#8 is the subject of this study as a second test system. ShC-D8 shown in **Fig. 4** [25]. There are 45 load points supplying various kinds of customers. The 0.4 kV low voltage customers are supplied via a 45 transformers point each of 22/0.415 kV, 500kVA transformers and the 22 kV customers are supplied directly. All feeder conductors are 3*240 mm^2AL. XLPE cables.

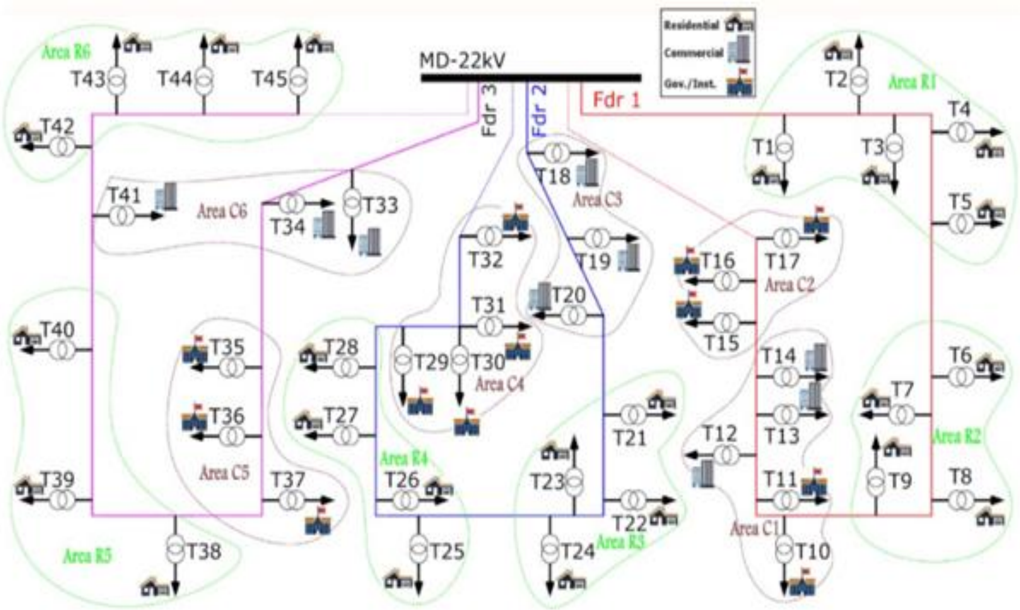

Fig. 4 ShC-D8 Distribution Test Systems [25].

4.2. Load Profiles and Cost Data

For all kind of customers, here two major classifications are made for deciding the load curve, residential and non-residential (government/institutions and commercial) customers. **Fig**.**5** shows the daily load curve for residential and non-residential customers [25]. For real system in Egypt, Egyptian daily load is considered [25] which are given in **Fig.6** to achieve more realistic results for this system.

The cost of electricity also varies over time during a day and is also dependent on the season. To study economic benefit of EV penetration in distribution system, time varying cost data is assumed. This data is extracted ON LINE from Nord Pool website [25] and gives the variation of cost over one particular day as shown in **Fig.7**. The energy cost can be calculated by the cumulative multiplication of the cost variation (in **Fig.7**) and energy variation curve corresponding to the calculated cost required (such as operation, and charging energy curves).

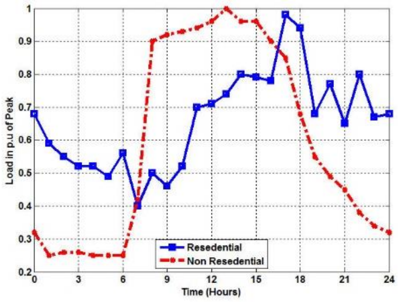

Fig. 5 Daily Load Curve

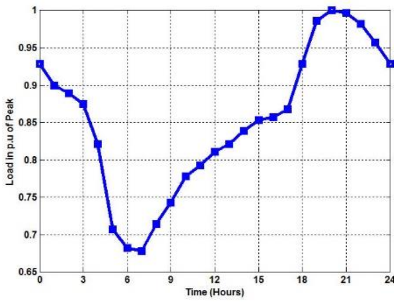

Fig. 6 Egyption Daily Load Curve

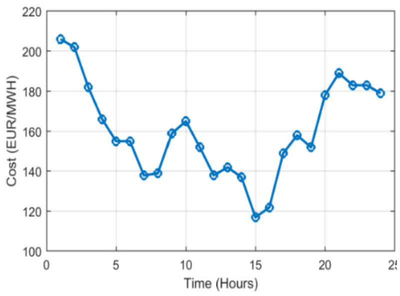

Fig. 7 Hourly Cost Data [at 26/6/2022]

4.3. EV Integration

The EVs load dependent on the number of customers, the penetration level, and the charging strategy for uncoordinated or coordinated charging.

4.3.1. Penetration level

Table 1 shows the peak load, number of customers and total EVs load in each bus with different penetration level 10%, 20%, 50% and 100%

Table 1 peak load and EVs load at all buss

Bus	Peak Load	Customers	Penetration Level (%)				Total EVs	Penetration Level (%)			
No.	LP	No.	10	20	50	100	P	10	20	50	100
	kW	N	N				kW	KW			
1	308.4	120	12	24	60	120	360	36	72	180	360
2	359.8	140	14	28	70	140	420	42	84	210	420
3	359.8	140	14	28	70	140	420	42	84	210	420
4	334.1	130	13	26	65	130	390	39	78	195	390
5	334.1	130	13	26	65	130	390	39	78	195	390
6	308.4	120	12	24	60	120	360	36	72	180	360
7	257	100	10	20	50	100	300	30	60	150	300
8	334.1	130	13	26	65	130	390	39	78	195	390
9	308.4	120	12	24	60	120	360	36	72	180	360
10	205.6	80	8	16	40	80	240	24	48	120	240
11	257	100	10	20	50	100	300	30	60	150	300
12	308.4	120	12	24	60	120	360	36	72	180	360
13	205.6	80	8	16	40	80	240	24	48	120	240
14	205.6	80	8	16	40	80	240	24	48	120	240
15	308.4	120	12	24	60	120	360	36	72	180	360
16	231.3	90	9	18	45	90	270	27	54	135	270
17	205.6	80	8	16	40	80	240	24	48	120	240
18	257	100	10	20	50	100	300	30	60	150	300
19	282.7	110	11	22	55	110	330	33	66	165	330
20	308.4	120	12	24	60	120	360	36	72	180	360
21	334.1	130	13	26	65	130	390	39	78	195	390
22	257	100	10	20	50	100	300	30	60	150	300
23	282.7	110	11	22	55	110	330	33	66	165	330
24	257	100	10	20	50	100	300	30	60	150	300
25	334.1	130	13	26	65	130	390	39	78	195	390
26	257	100	10	20	50	100	300	30	60	150	300
27	308.4	120	12	24	60	120	360	36	72	180	360
28	308.4	120	12	24	60	120	360	36	72	180	360
29	308.4	120	12	24	60	120	360	36	72	180	360
30	334.1	130	13	26	65	130	390	39	78	195	390
31	308.4	120	12	24	60	120	360	36	72	180	360
32	308.4	120	12	24	60	120	360	36	72	180	360
33	308.4	120	12	24	60	120	360	36	72	180	360
34	308.4	120	12	24	60	120	360	36	72	180	360
35	308.4	120	12	24	60	120	360	36	72	180	360
36	334.1	130	13	26	65	130	390	39	78	195	390
37	308.4	120	12	24	60	120	360	36	72	180	360
38	308.4	120	12	24	60	120	360	36	72	180	360
39	334.1	130	13	26	65	130	390	39	78	195	390
40	308.4	120	12	24	60	120	360	36	72	180	360
41	205.6	80	8	16	40	80	240	24	48	120	240
42	334.1	130	13	26	65	130	390	39	78	195	390
43	308.4	120	12	24	60	120	360	36	72	180	360
44	308.4	120	12	24	60	120	360	36	72	180	360
45	308.4	120	12	24	60	120	360	36	72	180	360

The numbers of vehicles that are considered in the test system depend on what scenario is being studied. There can be many cases ranging from 10% penetration to a 100% penetration. In **Fig.8** shows the EVs load for different penetrations of EVs and compares between this penetration levels in all buses of system.

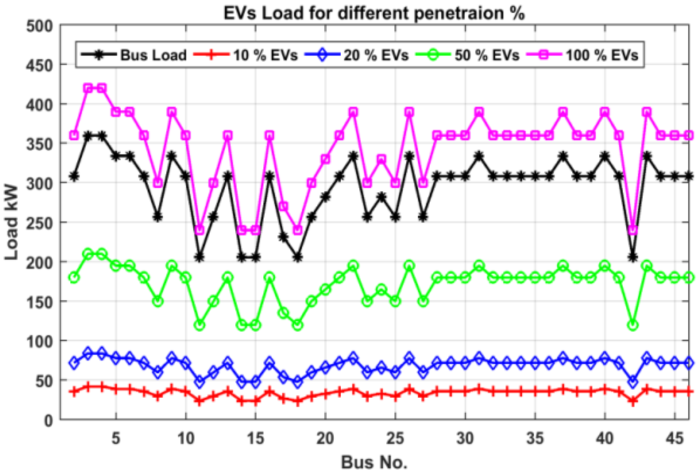

Fig. 8 EV Load for Different Penetration Level

4.3.2. EV Load for Uncoordinated Charging

In the uncoordinated charging scheme, the batteries of the EVs either start charging immediately when arrived at home and plugged in (usually during peak hours), or after user adjustable fixed start delay.[25]. In **Fig. 9** shown the EVs load uncoordinated charging at penetration level from 20% to 100%.

Fig. 10 and **Fig. 11** show the EVs load uncoordinated charging at bus 8 and bus 15 as for example for penetration level 20% and 100%, respectively.

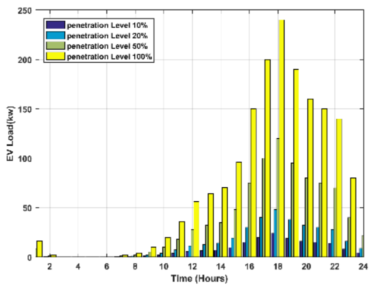

Fig. 9 EVs Load Uncoordinated For all penetration levels

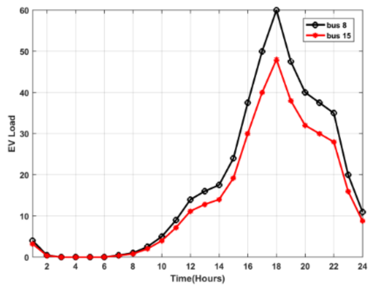

Fig. 10 EVs Load Uncoordinated For bus 8 and 15 at penetration level 20%

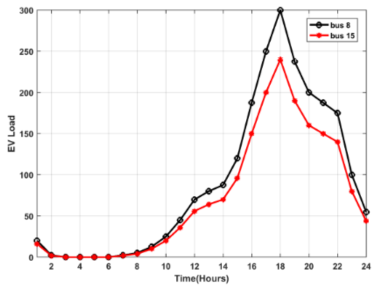

Fig. 11 EVs Load Uncoordinated For bus 8 and 15 at penetration level 100%

4.3.3. EV Load for Coordinating charging

EVs integration into distribution system can be improved when EVs charging at off-peak period this called coordinated charging; as shown in **Fig.12**, the EVs load uncoordinated charging at penetration level from 20% to 100%.

Fig. 13 and **Fig. 14** show the EVs load uncoordinated charging at bus 8 and bus 15 as for example at penetration level 20% and 100%, respectively.

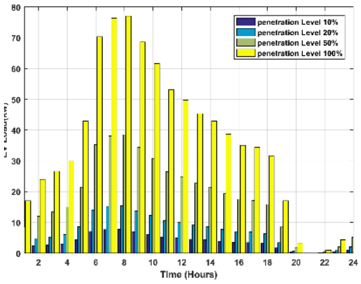

Fig.12 EVs Load Uncoordinated for all penetration levels

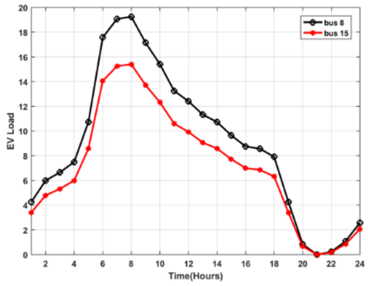

Fig.13 EVs Load Uncoordinated for bus 8 and 15 at penetration level 20%

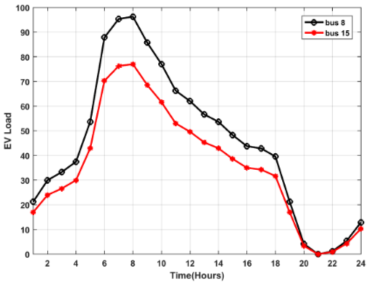

Fig.14 EVs Load Uncoordinated for bus 8 and 15 at penetration level 100%

4.4. Data of PV system

The following data of PV system in Table 2 is including the type of PV modules, the power , size of modules, and the cost from ENFSOLAR website (cost taken at 26/6/2022) [26]. The power is depended on the big size of EVCS in **Table 2**.

Table 2 Type of PV modules, price of items and the size of PV module

Type	Power (w)	At Irr.	Length (mm)	Width (mm)	Area (m^2)	Power (MW)	No.of Modules	Price (L.E/ item)	LE (million)	Area (m^2)	Length (mm)	Width (mm)
Poly-325W, Polycrystall	325	at 1000 W/m^2	1956	992	1.94	2.5	7692	890.5	6.850	14926	150	100
						2.5	7692		6.850	14926	150	100
						2	6154		5.480	11941	150	80

5. SIMULATION RESULTS

5.1. Optimal Location

Table 3 shows the best location of EVCS by using PSO technique and minimum losses; will notice the best locations are 13, 29 and 44.

Table 3 Best Location of EVCS using PSO technique

hour	Loc._1	Size_1	Loc._2	Size_2	Loc._3	Size_3
1	13.4029	0.93128	28.2124	1.52524	41.959	0.514491
2	11.3971	1.1616	29.9712	0.567688	44.4174	1.10017
3	11.719	0.609857	24.9337	1.41869	43.5205	0.618489
4	12.8795	1.12863	26.8454	1.34976	42.1246	0.656521
5	11.798	1.64571	22.8252	1.38608	43.9744	0.728664
6	12.5323	1.12041	31.5764	1.20568	42.0279	0.727613
7	11.9781	1.41265	30.1402	1.58865	43.9982	1.26998
8	12.59	1.88067	30.6607	1.82338	42.7549	1.61212
9	12.6215	1.7493	31.2649	2.28172	41.8117	1.50704
10	13.0892	1.87574	28.8289	1.99652	41.0742	2.26245
11	13.4215	1.96419	29.9923	1.96652	45.7828	1.53989
12	12.933	1.86714	26.1961	1.77888	43.8808	1.91474
13	11.8158	1.81564	28.0837	2.61519	41.0813	1.58299
14	14.2622	2.41533	29.3787	1.97073	39.9961	1.98847
15	12.186	1.96766	29.4972	2.53953	41.5618	2.51669
16	11.6161	1.55295	28.5111	1.98598	45.4108	1.68984
17	11.5517	2.4635	31.4705	2.69859	42.8603	1.59692
18	12.3934	2.35805	30.7768	1.74423	42.3034	2.68883
19	13.1924	2.07722	26.2251	1.85293	44.3405	2.04131
20	11.4028	2.63247	28.6785	1.81129	44.4433	1.17862
21	12.969	2.72013	29.4618	2.1368	40.7396	2.29825
22	11.3425	1.64642	29.4308	2.02837	43.6604	2.76822
23	9.76074	2.52209	28.4183	2.31101	42.2633	1.00207
24	12.2301	1.5194	27.8291	1.76547	42.5328	1.60189

5.2. Optimal sizing

In this section, the optimal sizing of EVCS is determined using PSO and AOA techniques, with different penetration EVs level 10%, 20%, 50%, and 100%, considering two objectives, which are minimum cost and minimum power losses, and using two strategies for coordinated charging and uncoordinated charging.

Table 4 shows the comparison between PSO technique and AOA technique to determine the optimal sizing of CS using the objective minimum cost.

In case coordinated charging and different penetration levels as shown **Fig. 15**, the cost by using AOA technique less than using PSO technique.

For example, the penetration level 10%: the cost using PS is 32890 EP/year , and using AOA technique is 32888 EP/year.
In case uncoordinated charging and different penetration levels as shown **in Fig. 16**, the cost by using AOA technique less than using PSO technique.
For example, the penetration level 10%: the cost using PSO technique is 33674 EP/year, and using AOA technique is 33673 EP/year.

Table 4 Optimal EVCS Sizing for Cost Minimization

PSO					AOA				
Coordinated					Coordinated				
	10%	20%	50%	100%		10%	20%	50%	100%
size1	2.1924	2.1258	2.2603	2.3996	size1	1.8622	1.9796	2.1843	2.0171
size2	2.4512	2.0093	2.193	2.4719	size2	2.0261	2.1989	2.2121	2.1961
size3	1.8001	1.6664	1.7845	1.965	size3	1.9621	1.6906	1.9555	1.825
min. cost	32890	33706	36157	40245	min. cost	32888	33705	36155	40242
Uncoordinated					Uncoordinated				
	10%	20%	50%	100%		10%	20%	50%	100%
size1	2.1435	2.2901	2.5	2.4791	size1	1.9574	1.936	2.4901	2.5
size2	2.1167	1.8911	2.3497	1.7526	size2	2.1655	2.055	2.4898	2.5
size3	2.0167	1.7328	1.5295	2.4717	size3	1.8444	2.0538	2.4479	2.5
min. cost	33674	35276	40087	48120	min. cost	33673	35274	40084	48115

Table 5 shows the comparison between PSO and AOA techniques to determine the optimal sizing of CS using the objective minimum power losses.
In case coordinated charging and different penetration levels as shown **Fig. 17**, the power losses using AOA technique less than using PSO technique.
For example, the penetration level 10%: the power losses using PSO = 0.3612 MW, and using AOA = 0.3516 MW.
In case uncoordinated charging and different penetration levels as shown **Fig. 18**, the power losses using AOA technique less than using PSO technique.
For example, the penetration level 10%: the power losses using PSO = 0.3775 MW, and using AOA = 0.3668 MW.

Table 5 Optimal EVCS Sizing for Power Losses Minimization

PSO					AOA				
Coordinated					Coordinated				
	10%	20%	50%	100%		10%	20%	50%	100%
size1	1.9058	1.8061	2.1054	2.4556	size1	1.9244	1.8982	2.1343	2.1779
size2	2.0217	1.6963	1.7062	2.4515	size2	1.8147	2.0225	1.9974	2.2718
size3	1.5662	1.9209	1.7491	1.9513	size3	1.2911	1.4604	1.5087	1.9128
Min.losses	0.3612	0.3648	0.3818	0.4305	min.losses	0.3516	0.3540	0.3673	0.4099
Uncoordinated					Uncoordinated				
	10%	20%	50%	100%		10%	20%	50%	100%
size1	2.058	1.6957	2.3271	2.4894	size1	1.9533	2.0602	2.3125	2.3816
size2	2.0052	1.9358	2.3024	2.3347	size2	1.989	2.0962	2.2764	2.3546
size3	1.4323	1.8894	1.8764	2.0088	size3	1.523	1.5474	1.8832	1.8344
Min.losses	0.3775	0.4011	0.5008	0.7631	min.losses	0.3668	0.3881	0.4809	0.7316

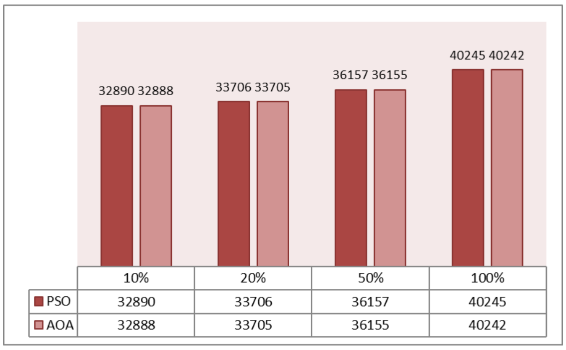

Fig. 15 The total energy cost at coordinated charging

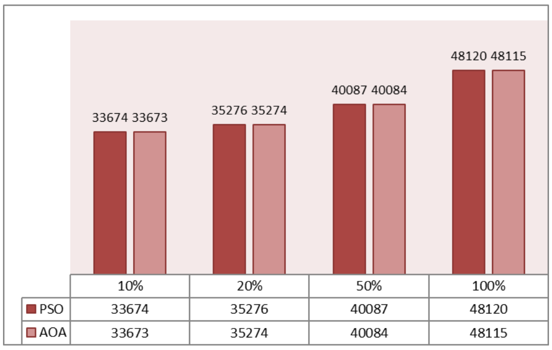

Fig. 16 The total energy cost at uncoordinated charging

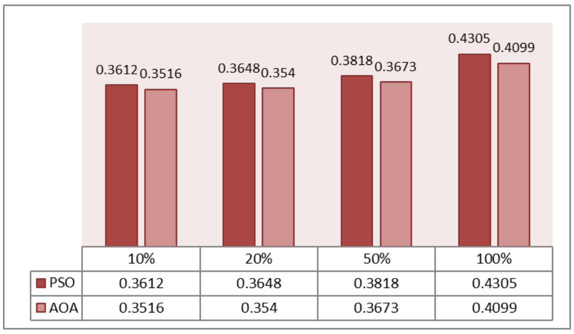

Fig. 17 The total power losses at coordinated charging

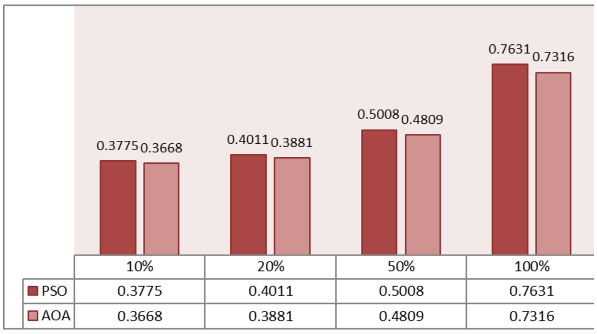

Fig. 18 The total power losses at uncoordinated charging

Fig. 19 shows the cost using PSO technique in cases coordinated and uncoordinated charging with different penetration levels, when controlled in number of EV.

For example, at penetration level, 20% the cost in coordinated charging is 33706 EP/year and the cost in uncoordinated charging is 35276 EP/year. The reduction of cost 1570 EP/year is 4.45%.

In **Fig. 20** shows the cost by using AOA technique in cases coordinated and uncoordinated charging with different penetration levels, when controlled in number of EV.

For example, at penetration level 20%, the cost in coordinated charging is 33705 EP/year and the cost in uncoordinated charging is 35274 EP/year. The reduction of cost 1569 EP/year is 4.44%.

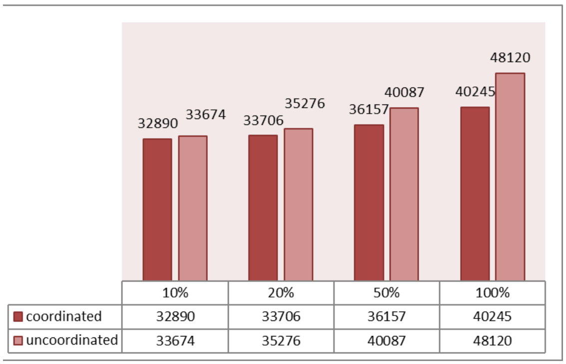

Fig. 19 The total energy cost at different charging strategy using PSO technique

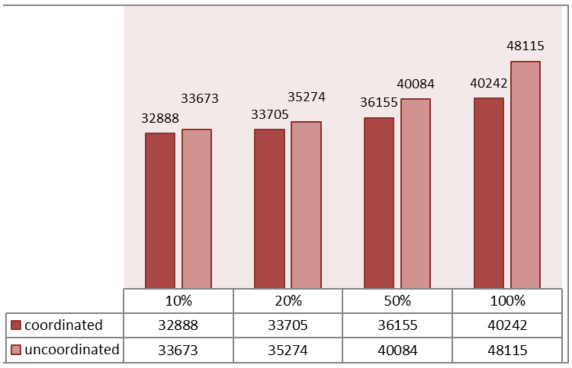

Fig. 20 The total energy cost at different charging strategy using AOA technique

Fig. 21 shows the power losses using PSO technique in cases coordinated and uncoordinated charging with different penetration levels, when controlled in number of EV.

For example, at penetration level 20% the power losses in coordinated charging is 0.3648 MW and in uncoordinated charging is 0.4011 MW.

In **Fig. 22** shows the power losses using AOA technique in cases coordinated and uncoordinated charging with different penetration levels, when controlled in number of EV.

For example, at penetration level 20% the power losses in coordinated charging is 0.354 MW and in uncoordinated charging is 0.3881 MW.

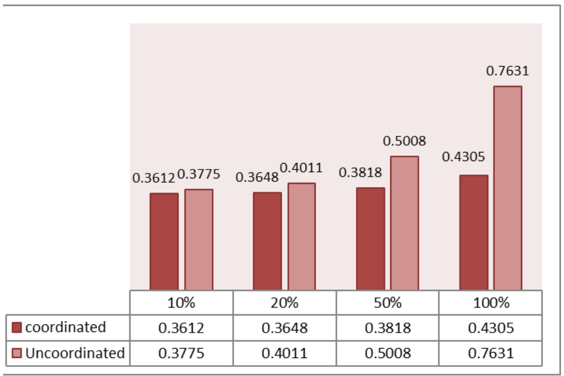

Fig. 21 The total power losses at different charging strategy using PSO technique

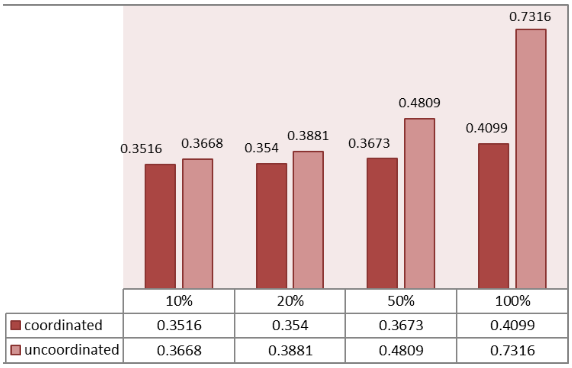

Fig.22 The total power losses at different charging strategy using AOA technique

5.2.1. Uncoordinated Charging

Fig. 23, 24, and 25 show the voltage profile in bus 18, 33, and 46 are cases of uncoordinated charging with different penetration level, respectively.

From these figures, when the penetration levels are increased, the voltage profile decreases. From example, in figure 24 shows the voltage profile at bus 33 uncoordinated charging with penetration level 10%, 20%, 50%, and 100% in the worst case hour 18:00. In case penetration level 10%, the voltage is 0.99813 p.u, in penetration level 20%, the voltage is 0.9979 p.u, in penetration level 50% the voltage is 0.9974 p.u, and in penetration level 100% the voltage is 0.9965 p.u.

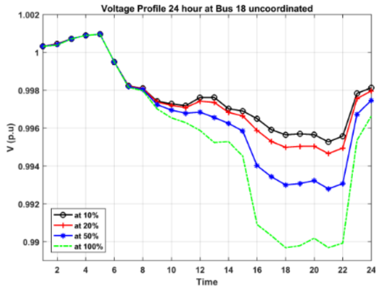

Fig. 23 Voltage profile at bus 18 Uncoordinated charging

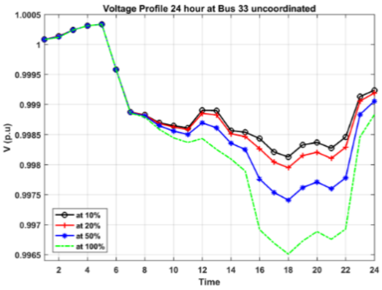

Fig. 24 Voltage profile at bus 33 Uncoordinated charging

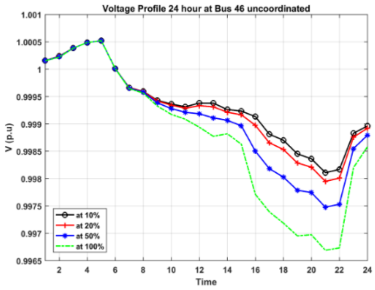

Fig. 25 Voltage profile at bus 46 Uncoordinated charging

5.2.2. Coordinated Charging

Fig. 26, 27, and 28 show the voltage profile in bus 18, 33, and 46 are cases of coordinated charging with different penetration level, respectively.

From these figures, when the penetration levels are increased the voltage profile decreases. From example, in **Fig.** 27 shows the voltage profile at bus 33 coordinated charging with penetration level 10%, 20%, 50%, and 100% in the worst case hour 9:00. In case penetration level 10% the voltage is 0.9987 p.u, in penetration level 20%, the voltage is 0.9985 p.u, in penetration level 50% the voltage is 0.9983 p.u, and in penetration level 100% the voltage is 0.9979 p.u.

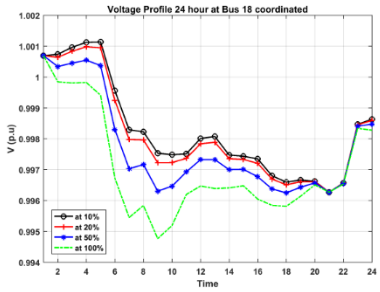

Fig. 26 Voltage profile at bus 18 coordinated charging

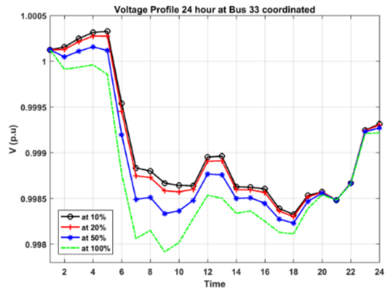

Fig. 27 Voltage profile at bus 33 coordinated charging

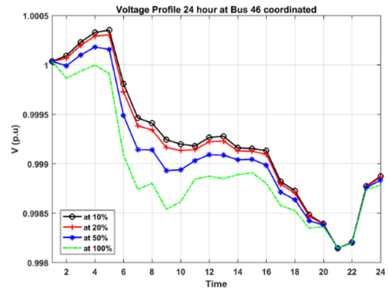

Fig. 28 Voltage profile at bus 46 coordinated charging

The coordinated charging strategy gives the best result for voltage profile compared with uncoordinated charging strategy. For example, at hour 18:00, **Fig. 27** the voltage profile at bus 33 with coordinated charging, in penetration level 100%, the voltage is 0.9981p.u which is better than the voltage profile in **Fig. 24** at the same bus and same penetration level the voltage is 0.9965p.u.

5.2.3. Comparison results between PSO and AOA techniques

In this section, the comparison results between PSO and AOA using two strategies charging coordinated and uncoordinated, and two case of penetration level:

Case 1: 20% Penetration level of EVs; This means that 20% of the total consumers use an electric vehicle.

Case 2: 100 % Penetration level of EVs; this means that 100% of the total consumers use an electric vehicle, at three buss 18, 33, and 46.

At bus 18:

Fig. 29 shows the voltage profile at base case (before sizing the EVCS), when determine the sizing of EVCS and using two optimization technique PSO and AOA techniques, The voltage profile at AOA technique is better than voltage profile at base case and PSO technique. For example, the worst case at hour 18:00, in AOA technique the voltage is 0.9848 p.u, in PSO the voltage is 0.9842 p.u, and in base case the voltage is 0.9774p.u. **Fig. 30** shows the voltage profile at penetration level 20%, the strategies charging coordinated and uncoordinated, the results of AOA technique is better than the resulte of PSO technique, where the result in worst case at hour 21:00 for coordinated charging, the AOA technique voltage is 0.9963 p.u and the PSO technique voltage is 0.9959 p.u. And for uncoordinated charging, the AOA technique voltage is 0.995 p.u and the PSO technique voltage is 0.993p.u. **Fig.31** shows the voltage profile at penetration level 100%, the strategies charging coordinated and uncoordinated the results of AOA technique are better than the results of PSO, where the result in worst case at hour 9:00 for coordinated charging, the AOA technique voltage is 0.9948 p.u and the PSO technique voltage is 0.9944 p.u. And in worst case at hour 18:00 for uncoordinated charging, the AOA technique voltage is 0.99 p.u and the PSO technique voltage is 0.98 p.u.

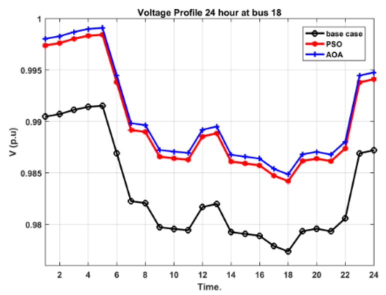

Fig. 29 Voltage profile at bus 18 Before the sizing of EVCS

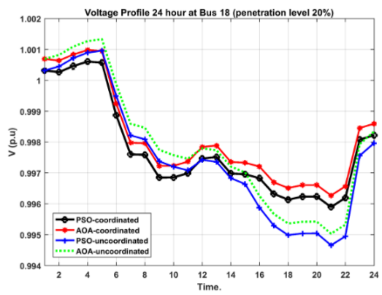

Fig. 30 Voltage profile at bus 18 with 20% penetration EVs

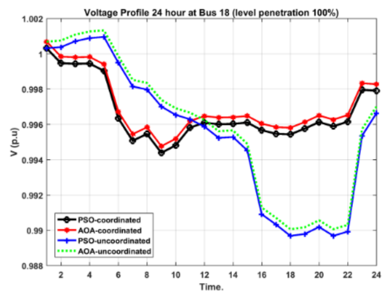

Fig. 31 Voltage profile at bus 18 with 100% penetration EVs

At bus 33:

Fig. 32 shows the voltage profile at base case (before sizing the EVCS), when determine the the sizing of EVCS and using two optimization technique PSO and AOA techniques. The voltage profile at AOA technique is better than voltage profile at base case and PSO. For example, the worst case at hour 18:00, in AOA technique the voltage is 0.989p.u, in PSO the voltage is 0.988p.u, and in base case the voltage is 0.982 p.u. **Fig. 33** shows the voltage profile at penetration level 20%, the strategies charging coordinated and uncoordinated, the results of AOA technique are better than the resulte of PSO technique, where the result in worst case at hour 18:00 for coordinated charging, the AOA technique voltage is 0.9983 p.u and the PSO technique voltage is 0.9982 p.u. And for uncoordinated charging, the AOA technique voltage is 0.9982 p.u and the PSO voltage is 0.9979p.u. **Fig. 34** shows the voltage profile at penetration level 100%, the strategies charging coordinated and uncoordinated the results of AOA technique are better than the results of PSO, where the result in worst case at hour 9:00 for coordinated charging, the AOA technique voltage is 0.9978 p.u and the PSO technique voltage is 0.998 p.u. And in worst case at hour 18:00 for uncoordinated charging, the AOA technique voltage is 0.9966 p.u and the PSO voltage is 0.9965 p.u.

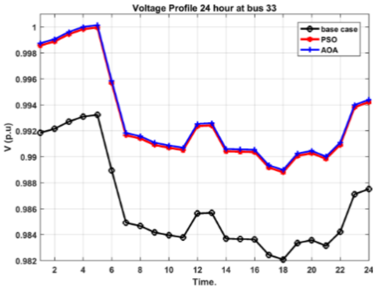

Fig. 32 Voltage profile at bus 33 Before the sizing of EVCS

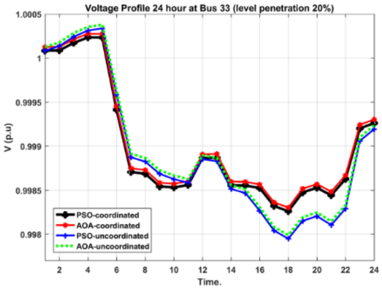

Fig. 33 Voltage profile at bus 33 with 20% penetration level of EVs

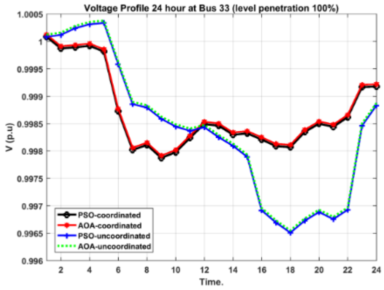

Fig. 34 Voltage profile at bus 33 with 100% penetration level of EVs

<u>At bus 46:</u>

Fig. 35 shows the voltage profile at base case (before sizing the EVCS), when determine the the sizing of EVCS using two optimization technique PSO and AOA techniques. The voltage profile at AOA technique is better than voltage profile at base case and PSO technique. For example, the worst case at hour 21:00, in AOA technique the voltage is 0.991 p.u, in PSO the voltage is 0.99 p.u, and in base case the voltage is 0.985p.u. **Fig. 36** shows the voltage profile at penetration level 20%, the strategies charging coordinated and uncoordinated the results of AOA technique are better than the results of PSO, where the result in worst case at hour 21:00 for coordinated charging, the AOA technique voltage is 0.9983p.u and the PSO voltage is 0.9981p.u. And for uncoordinated charging, the AOA technique voltage is 0.9982 p.u and the PSO technique voltage is 0.9978 p.u. **Fig. 37** shows the voltage profile at penetration level 100%, the strategies charging coordinated and uncoordinated results of AOA technique are better than the resulte of PSO, where the result in worst case at hour 21:00 for coordinated charging, the AOA technique voltage is 0.9983p.u and the PSO technique voltage is 0.9982 p.u. And in worst case at hour 21:00 for uncoordinated charging, the AOA technique voltage is 0.9966 p.u and the PSO technique voltage is 0.9967 p.u.

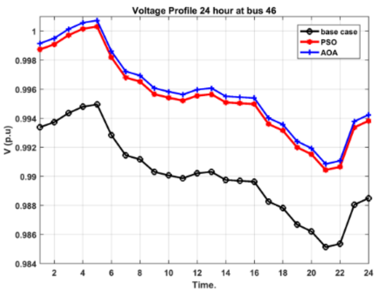

Fig. 35 Voltage profile at bus 46 Before the sizing of EVCS

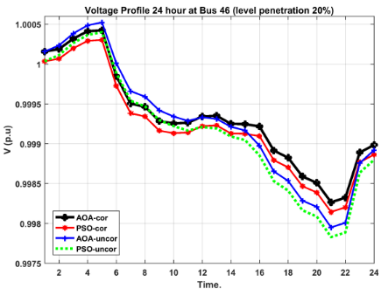

Fig. 36 Voltage profile at bus 46 with 20% penetration level of EVs

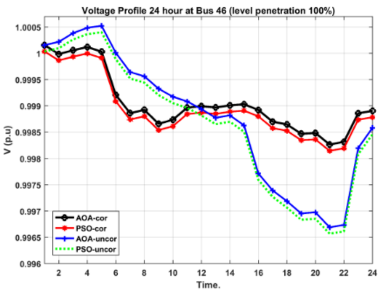

Fig. 37 Voltage profile at bus 46 with 100% penetration level of EVs

1. SUMMARY AND CONCLUSIONS

This paper introduces a study and analysis on EVCS optimal allocations problem. The problem has been solved using to heuristic techniques AOA and PSO. The objective functions have been minimizing power losses and minimizing costs. In this work the handle EVCS locations and capacities for optimal configuration as well as keeping the voltage profile within a preset voltage levels as demanded. The optimal configuration schemes ensure the system operates in an optimal state in the sense of at acheving the objective functions and maintaining voltage profile. Comparing the results of AOA with PSO techniques in this paper have been done. AOA technique has faster convergence speed, shorter running time and more accurate results compared to PSO technique. The results show that the AOA has better performance than PSO technique in solving the EVCS configuration problem.

REFERENCES

[1] Fazelpour F, Vafaeipour M, Rahbari O, Rosen MA., " Intelligent optimization to integrate a plug-in hybrid electric vehicle smart parking lot with renewable energy resources and enhance grid characteristics," Energy Conversion and Management, vol. 77,pp. 250–261, January.2014.

[2] International energy outlook 2011: energy information administration (EIA), office of integrated analysis and forecasting, U.S. Department of energy, Washington DC, 2011.

[3] Amini MH, et al., “Effect of electric vehicle parking lot’s charging demand as dispatchable loads on power loss,” IEEE international conference on electro information technology (EIT), 19-21 May. 2016.

[4] J. Garcia-Guarin, W. Infante, . Ma, D. Alvarez, S. Rivera, “Optimal scheduling of smart microgrids considering electric vehicle battery swapping stations,” International Journal of Electrical and Computer Engineering (IJECE), vol. 10, no. 5, October 2020, pp. 5093~5107.

[5] A. Geetha, C. Subramani, "A significant energy management control strategy for a hybrid source EV," International Journal of Electrical and Computer Engineering (IJECE), vol. 9, no. 6, December 2019, pp. 4580~4585.

[6] Kempton W, Amardeep Dhanju, "Electric vehicles with V2G," windtech international, vol. 18, no. 2, 2006.

[7] Kempton W, Tomic J, “Vehicle-to-grid power fundamentals: Calculating capacity and net revenue,” journal of power sources, vol. 144, no. 1, pp. 268-279, 2005.

[8] Amini MH, et al, “ARIMA-based demand forecasting method considering probabilistic of electric vehicle’s parking lots,” power and energy and energy society general meeting, IEEE, 26-30 July. 2015.

[9] J. de Hoog et al, “The importance of spatial distribution when analysing the impact of electric vehicles on voltage stability in distribution networks,” energy system, vol. 6, no. 1, pp. 63–84, 2014.

[10] Ehsani M, Falahi M, Lotfifard S, “Vehicle to grid services: potential and applications,” energies, vol. 5, no. 10, pp. 4076-4090, 2012.

[11] Honarmand M, Zakariazadeh A, JadidSh, “Self-scheduling of electric vehicles in an intelligent parking lot using stochastic optimization,” journal of the franklin institute, vol. 352, no. 2, pp. 449-467, 2015.

[12] Liu Z, Wen F, Ledwich G, “Optimal planning of electric-vehicle charging stations in distribution systems,” IEEE transactions on power delivery, vol. 28, no. 1, pp. 102–110, January. 2013.

[13] Mohamed Abdelhamed Zaki, Tarek Mahmoud, Mohamed Atia, ELsaid Abd Elaziz Osman “Optimal sizing and sitting of electirc vehicle charging station by using archimedes optimization algorithm technique,” International Journal of Power

Electronics and Drive System (IJPEDS), vol. 12, no. 4, pp. 2557–2569, December. 2021.

[14] Liang Chen, Chunxiang Xu, Heqing Song, Kittisak Jermsittiparsert, “Optimal sizing and sitting of EVCS in the distribution system using metaheuristics: A case study,” Energy Reports, ElSEVIER, vol. 7, pp. 208–217, November. 2021.

[15] Yingliang Li , Hao Zhu, Deming Wang, Kang Wang, Weixu Kong, and Xiaomeng Wu, “Comprehensive optimization of distributed generation considering network reconstruction based on Archimedes optimization algorithm,” IOP Conf. Series: Earth and Environmental Science 647 (2021) 012031, ICAESEE 2020.

[16] Ziad M. Ali, Ibrahim Mohamed Diaaeldin, Ahmed El-Rafei, Hany M. Hasanien, Shady H.E. Abdel Aleem and Almoataz Y. Abdelaziz, “A novel distributed generation planning algorithm via graphically-based network reconfiguration and soft open points placement using Archimedes optimization algorithm,” Ain Shams Engineering Journal.

[17] C. Mouli, P. Bauer, M. Zeman, " Comparison of system architecture and converter topology for a solar-powered electric vehicle charging station," In 2015 9th International Conference on Power Electronics and ECCE Asia (ICPE-ECCE Asia), pp. 1908-1915, 2015.

[18] P. Goli and W. Shireen, "PV powered smart charging station for PHEVs," Renewable Energy, vol. 66, pp. 280-287, 2014.

[19] Gamboa, C. Hamilton, R. Kerley, S. Elmes, A. Arias, J. Shen, I. Batarseh, "Control strategy of a multi-port, grid-connected, direct-DC PV charging station for plug-in electric vehicles," In 2010 IEEE Energy Conversion Congress and Exposition, pp. 1173-1177, 2010.

[20] F. Fattori, N. Anglani, G. Muliere, "Combining photovoltaic energy with electric vehicles, smart charging, and vehicle-to-grid," Solar Energy, vol. 110, pp. 438-451, 2014.

[21] O. Hafez and K. Bhattacharya, "Optimal design of electric vehicle charging stations considering various energy resources," Renewable Energy, vol. 107, pp. 576-589, 2017.

[22] G. C. Mouli, P. Bauer, M. Zeman, M. "System design for a solar-powered electric vehicle charging station for workplaces," Applied Energy, vol. 168, pp. 434-443, 2016.

[23] W. Khan, F. Ahmad, M. S. Alam, "Fast EV charging station integration with grid ensuring optimal and quality power exchange," Engineering Science and Technology, vol. 22(1), pp. 143-152, 2019.

[24] A. Domínguez-Navarro, et al., "Design of an electric vehicle fast-charging station with integration of renewable energy and storage systems, "International Journal of Electrical Power & Energy Systems, vol. 105, pp. 46-58, 2019.

[25] Ahmed R. Abul'Wafa, Aboul’Fotouh El’Garably, Wael A.Fatah Mohamed, “Impacts of Uncoordinated and Coordinated Integrationof Electric Vehicles on Distribution SystemsPerformance,” 2017 Nineteenth International Middle East Power Systems Conference (MEPCON), Menoufia University, Egypt, December 2017.

[26] https://www.enfsolar.com/pv/panel?gclid=EAIaIQobChMI3vj0dXN7gIV1OvtCh3H6wPEEAAYAiAAEgI39PD_BwE.